Supporting Information

Topological insulator bismuth selenide with unique cloud-like hollow structure as a bidirectional electrocatalyst for robust lithium-sulfur batteries

Mincai Zhao[a,1], Junjie Fu[a,1], Daoping Cai[a,*], Chaoqi Zhang[a], Ban Fei[a,c], Yinggan Zhang[b,*], Baisheng Sa[a], Qidi Chen[a], and Hongbing Zhan[a]

[a] College of Materials Science and Engineering, Fuzhou University, Fuzhou, 350108, China.

[b] College of Materials Science and Engineering, Xiamen University, Xiamen, 361005, China.

[c] School of Chemistry, Trinity College Dublin, Dublin 2, Ireland.

*Corresponding authors: Daoping Cai, and Yinggan Zhang.

E–mail addresses: dpcai@fzu.edu.cn, and ygzhang@xmu.edu.cn.

Experimental Section

1.1. Synthesis of BiOBr nanobelts

The synthesis of BiOBr nanosheets was carried out as follows, where 0.2 g of polyethylene glycol was dissolved in a mixture solution of 10 mL of ethanol and 10 mL deionized water and stirring for 2 min. Then 1.0 mg of bismuth nitrate pentahydrate ($Bi(NO_3)_3 \cdot 5H_2O$) and 0.4 mL hydrogen bromide (HBr) were added. After 5 min stirring, the mixture solution was transferred into a 25 mL Teflon-lined autoclave with a stainless-steel shell and kept at 160 °C for 6 h. The product was collected after centrifugation, thoroughly washed with deionized water and ethanol several times, and finally dried in an oven at 60 °C for overnight.

1.2. Synthesis of Bi_2S_3 and BiSe

Typically, 7.8 mg of selenium powder and 20 mg of as-synthesized BiOBr nanosheets were dispersed in a mixture solution of 3 mL hydrazine hydrate and 20 mL deionized water, and then transferred into a 25 mL Teflon-lined autoclave with a stainless-steel shell and kept at 165 °C for 12 h. After cooling naturally, the Bi_2Se_3 was collected after centrifugation, thoroughly washed with deionized water and ethanol several times, and finally dried in an oven at 60 °C for overnight. The BiSe went through the same process by changing the amount of the selenium powder to 5.2 mg.

1.3. Synthesis of KB/S cathode

The KB/S composite was prepared by the melt-diffusion method. The KB mixed with sublimed sulfur (weight ratio of 1:3) were place into a sealed glass bottle and the KB/S composite was obtained after heating at 155 ℃ for 12 h. The KB/S composite cathode was prepared by the slurry-coating method. The slurry was prepared by mixing KB/S composites, KB, and PVDF with a mass ratio of 8:1:1 in NMP. The slurry was then spread on carbon coated aluminum foil and dried in a vacuum oven at 60 ℃ for 6 h, then the carbon coated aluminum foil with dried slurry was punched into circle disks with a parameter of 12 mm. The areal sulfur loading for each disk was controlled around 1.0 mg cm^{-2}.

1.4. Preparation of the Bi_2Se_3 modified separator

The Bi_2Se_3 layer uniformly coated on a separator was obtained by the vacuum filtration method. 4.2 mg of Bi_2Se_3, 1.2 mg of PVDF and 0.6 mg of rGO were dispersed in 10 mL NMP by sonication for 2 h to obtain a homogeneous suspension, which was filtered through a polypropylene (PP) membrane (Celgard 2400), the obtained functionalized separator was dried at 60 ℃ overnight under vacuum. Eventually, the coated separator was cut into discs with a diameter of 19 mm. BiSe coated separator was prepared using the same method. The mass loading of the modified materials were controlled at about 0.6 mg cm^{-2}.

1.5. Lithium polysulfide (Li_2S_6) solution and visualized adsorption test

0.1 M Li_2S_6 solution was prepared by dissolving S and Li_2S (the molar ratio was 5:1) in a mixed solvent of 1,2-dimethoxyethane (DME) and 1,3-dioxolane (DOL) (v/v =1:1) under vigorous stirring at 70 ℃ for 24 h. Then 20 mg Bi_2Se_3 and BiSe were put

into 3 mL Li_2S_6 solution for visualized adsorption test. All the above operations were carried out in an argon-filled glove box.

1.6. Symmetric cell assembly and kinetic evaluation of polysulfide conversion

0.25 M Li_2S_6 electrolyte was prepared by vigorous stirring S and Li_2S (the molar ratio is 5:1) in the electrolyte (1 M bis(trifluoromethanesulfonyl)imide lithium salt (LiTFSI) in DOL/DME (v:v =1:1)) at 70 ℃ for 24 h. The electrode was prepared by mixing active materials (Bi_2Se_3 and BiSe) and PVDF with a weight ratio of 9:1 in NMP solvent followed by coating the slurry onto Al foil. Two identical electrodes were used as the working and the counter electrodes with a mass loading of 1.0 mg cm^{-2}, and 40 μL of Li_2S_6 (0.25 M) was used as electrolyte. The CV measurements of the symmetric cells were tested measured by electrochemical workstation (CHI660E) with a voltage window between −1.0 to 1.0 V at scan rates of 1, 3, 5 and 10 mV s^{-1}.

1.7. Li_2S nucleation and decomposition measurements

For the study of liquid-solid conversion kinetics, Li_2S_8 solution (0.5 M) was prepared by mixing S and Li_2S (molar ratio of 7:1) and dissolving the mixture in DME and DOL (v/v = 1:1) solution containing 1.0 M LiTFSI under vigorous stirring for 24 h. nucleation and decomposition experiments of Li_2S on different reactive surfaces were investigated in 2032-type coin cells with Celgard 2400 PP membrane as separator. Carbon papers (CP) were used as current collector to load the Bi_2Se_3 and BiSe, CP-Bi_2Se_3 and CP-BiSe were applied as cathodes and lithium foil was used as anode. 20 μL of Li_2S_8 (0.5 M) was dropped onto the cathode, and blank electrolyte with 1.0 M LiTFSI and 1 wt % $LiNO_3$ but without Li_2S_8 was dropped onto anode side.

For Li_2S nucleation, the cells were first discharged galvanostatically at 0.112 mA to 2.19 V and then kept potentiostatically at 2.05 V for Li_2S to nucleate until the current dropped below 10^{-2} mA for depositing and growth of Li_2S on various host surfaces. For Li_2S decomposition, the assembled cells were galvanostatically discharged to 1.70 V at 0.112 mA for complete transformation of LiPSs into solid Li_2S and then potentiostatically charged at 2.35 V until the charge current was below 10^{-2} mA for the oxidization process from solid Li_2S to soluble LiPSs.

1.8. Materials characterization

The information of composition, microstructure and morphology of the products were analyzed by X-ray diffractometer (XRD, Rigaku, D/max-UItima III difractometer, Cu Kα radiation, λ = 0.15418 nm), X-ray photoelectron spectroscopy (XPS, Thermo Fisher Scientific, ESCALAB 250), field emission scanning electron microscope (FESEM, Germany, Zeiss Supra 55), high-resolution transmission electron microscope (HRTEM, FEI, Talos F200i), the thermogravimetric analysis (TGA, NETZSCH, STA449-F5).

1.9. Electrochemical measurements

CR2032 coin cells were assembled in an Ar-filled glovebox (<0.5 ppm of O_2) by using the KB/S cathode, modified separators, and Li foil anodes. The electrolyte was bis(trifluoromethanesulfonyl)imide lithium (1 M) in a mixed solvent of 1,2-dimethoxyethane and 1,3-dioxolane (1:1, v/v) with $LiNO_3$ (1 wt.%). Galvanostatic charge and discharge tests were conducted on LAND CT2001A within a potential range from 1.7 to 2.8 V. The specific capacity was calculated based on the weight of

sulfur in each cell (1 C=1675 mA g^{-1}). Cyclic voltammetry curves and electrochemical impedance spectroscopy were measured by electrochemical workstation (CHI660E). CV curves were performed with the sweep rates from 0.1 to 0.4 mV s^{-1}. EIS profiles were tested with the frequency range from 10^{-2} to 10^{5} Hz.

1.10. Computational methods

Density functional theory (DFT) calculations presented in our work have been carried out by the Vienna *ab initio* Simulation Package (VASP) [S1,S2]. And the generalized gradient approximations (GGA) of Perdew-Burke-Ernzerhof (PBE) [S3] were used for the exchange-correlation functional [S4]. A cutoff energy of 500 eV was applied in all calculations. A vacuum space of 15 Å in the *z*-axis direction to avoid the interaction between repeated units were introduced. The binding energy (E_b) is defined as the energy difference of adsorbed model ($E_{Li_2S_n/sur}$) and the summation of pure Li_2S_n ($E_{Li_2S_n}$, n=1, 2, 4, 6, 8) molecule and the surface energy (E_{sur}) according to $E_b = E_{Li_2S_n/sur} - E_{sur} - E_{Li_2S_n}$ [S5]. The Gibbs free energy change (ΔG) was calculated by the equation: ΔG = ΔE + ΔZPE - TΔS, where ΔE was the change of total energy, ΔZPE was the difference of zero-point energy, T was 298.15 K, ΔS was the change of entropy, respectively. The zero-point energy and entropy from vibrational degrees of freedom were obtained with the fixed substrate. All the calculation models adopted in this work were conducted with the ALKEMIE platform [S6].

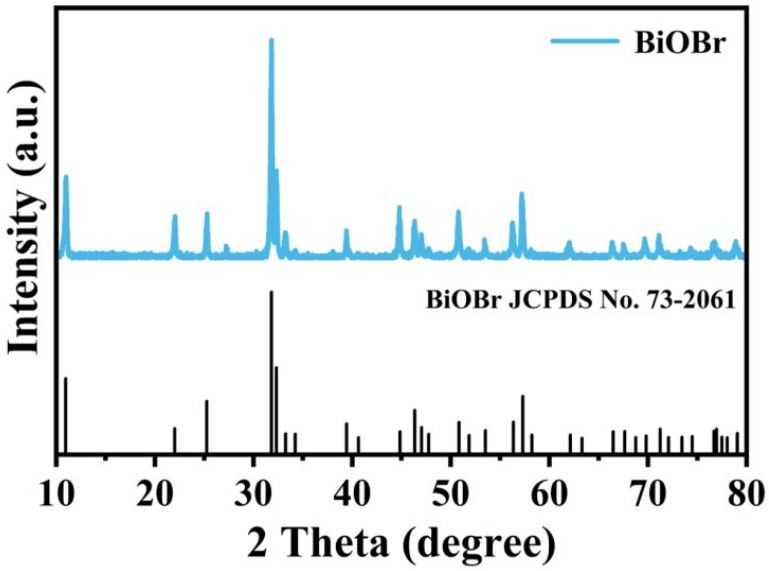

Fig. S1. (a) XRD of the BiOBr nanosheets.

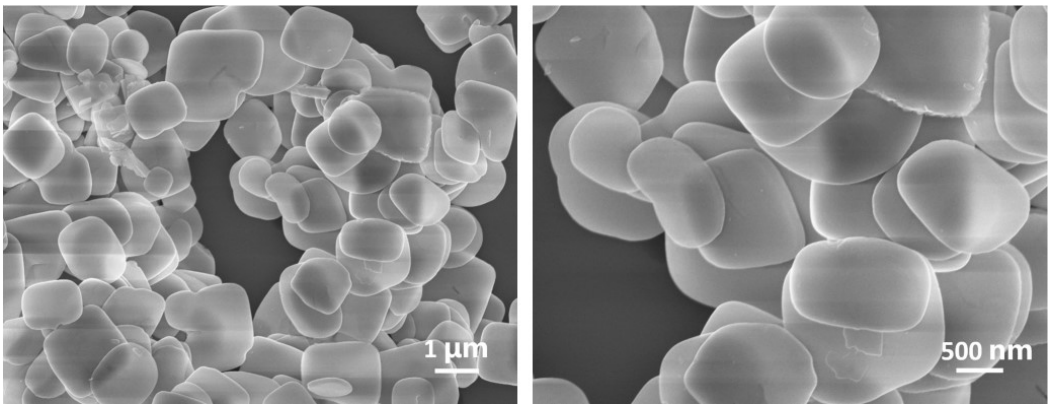

Fig. S2. SEM images of the BiOBr nanosheets.

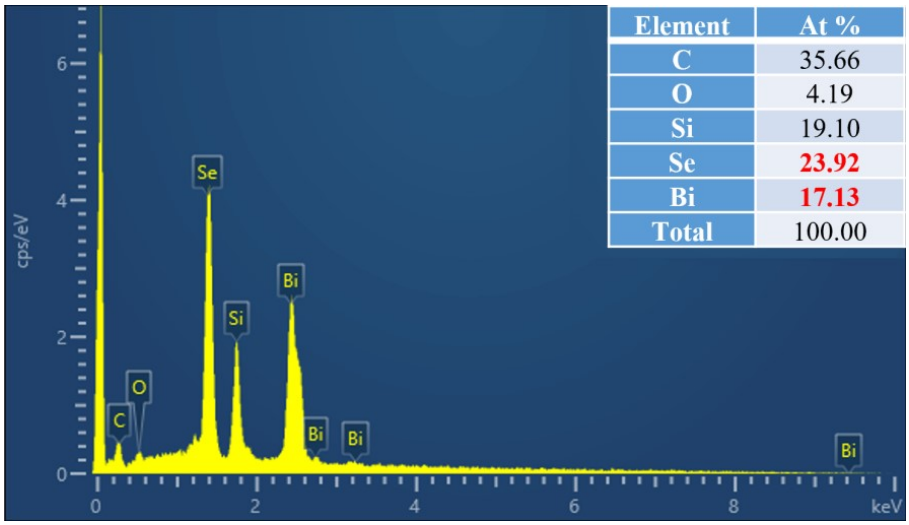

Fig. S3. EDS spectrum of the Bi_2Se_3.

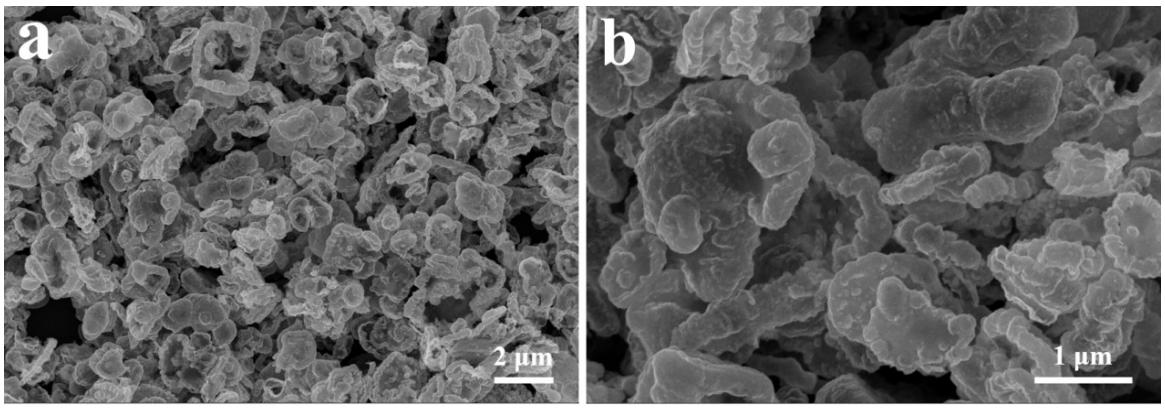

Fig. S4. SEM images of the BiSe.

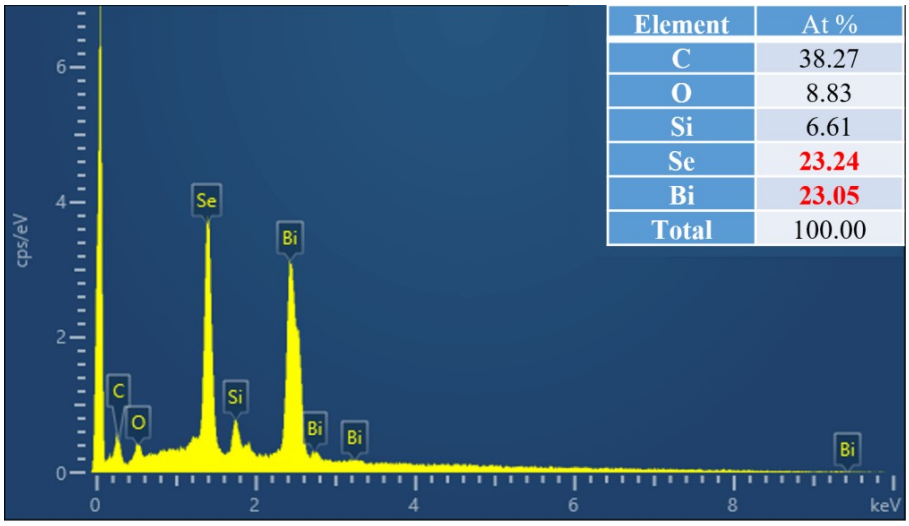

Fig. S5. EDS spectrum of the BiSe.

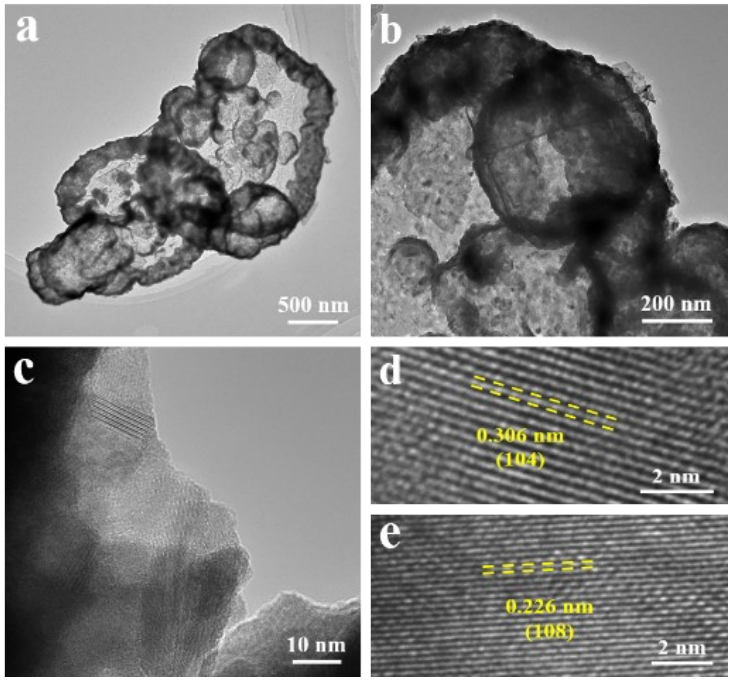

Fig. S6. (a, b) TEM and (c-e) HRTEM images of the BiSe.

Table S1. the actual content of Bi and Se in the Bi_2Se_3 and BiSe by ICP-OES.

Nominal composition	ICP-AES composition
Bi_2Se_3	$Bi_{2.14}Se_3$
BiSe	$Bi_{1.2}Se$

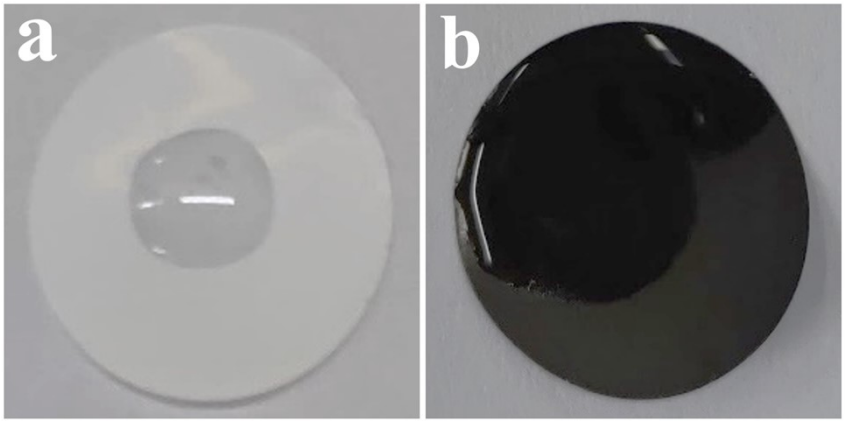

Fig. S7. Electrolyte wettability test of the Bi_2Se_3/PP separator.

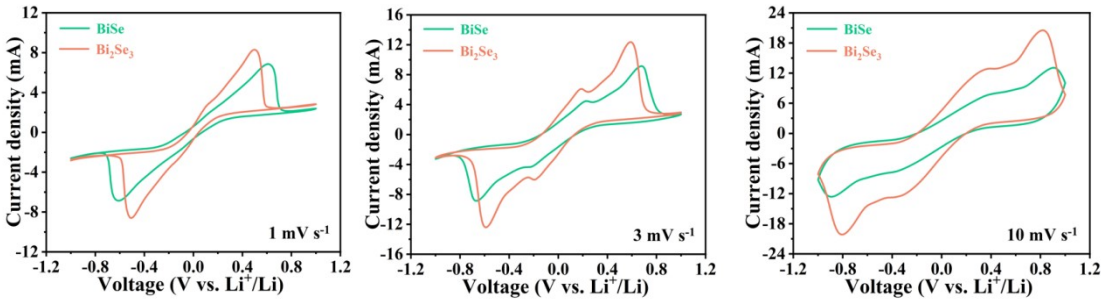

Fig. S8. CV curves of the Li_2S_6 symmetric cells with Bi_2Se_3 and BiSe under various scan rates.

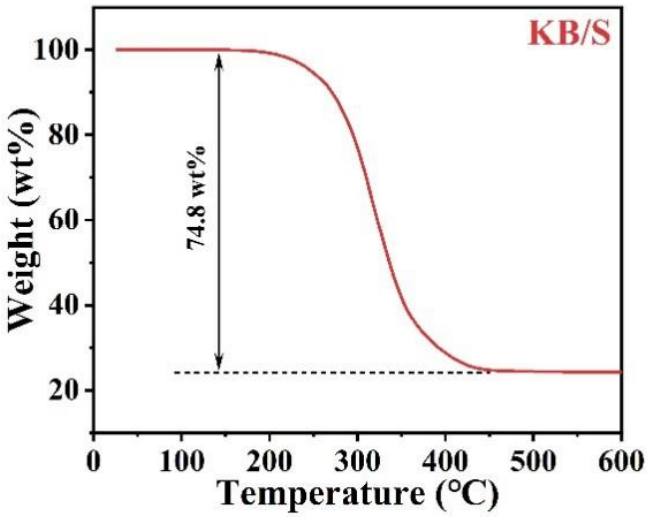

Fig. S9. TGA curve of the KB/S.

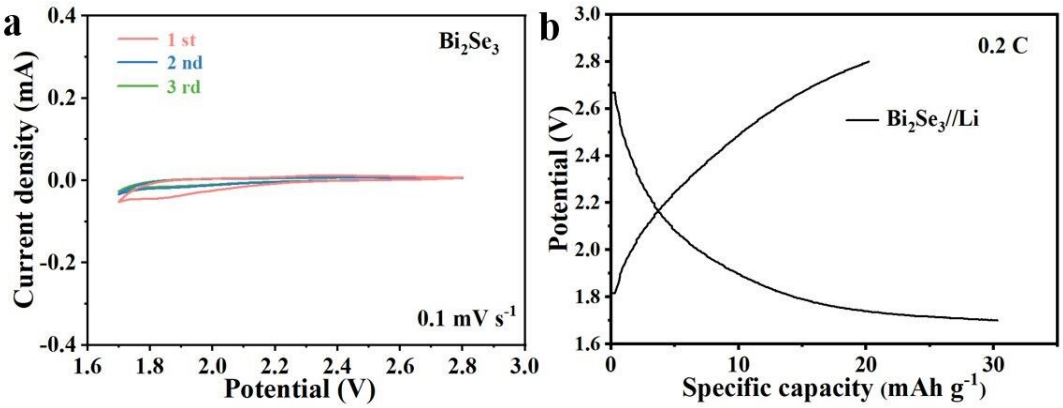

Fig. S10. (a) CV curves at 0.1 mV s^{-1} and (b) GCD curves at 0.2 C of the Bi_2Se_3//Li cell (without sulfur loading).

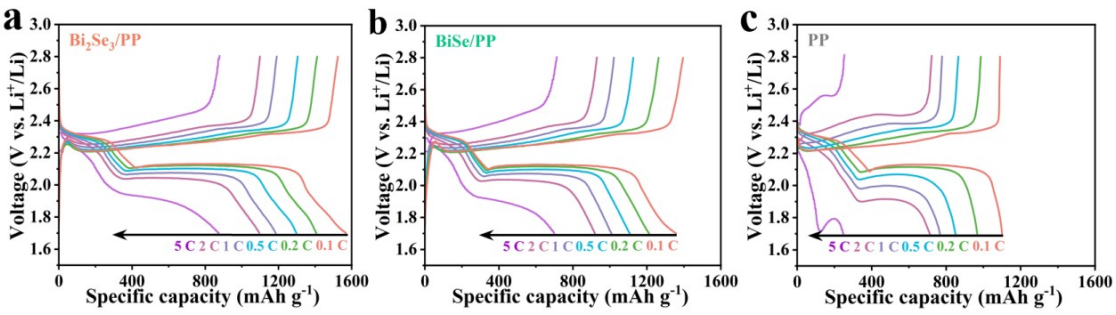

Fig. S11. GCD curves of batteries with (a) Bi_2Se_3/PP, (b) BiSe/PP and (c) PP separators.

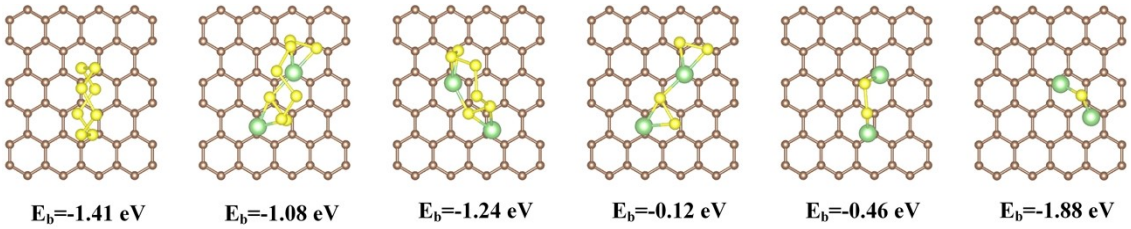

Fig. S12. Optimized geometries of S_8/Li_2S_x (x=1, 2, 4 , 6, 8) molecules adsorbed on graphene.

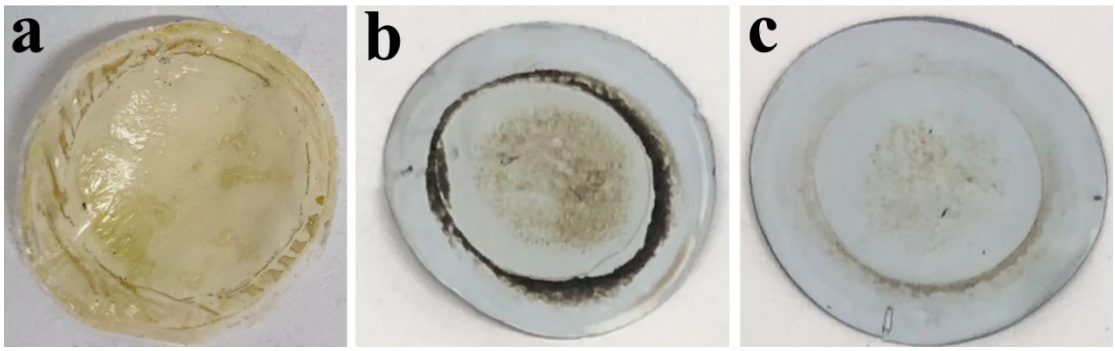

Fig. S13. Digital photos of (a) PP, (b) BiSe/PP, (c) Bi_2Se_3/PP after 100 cycles at 0.2 C.

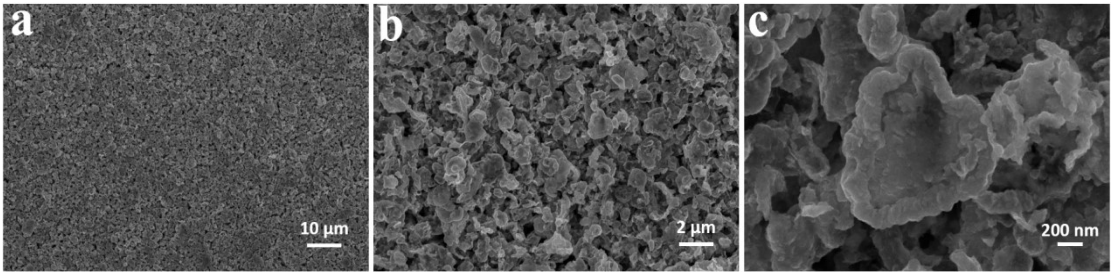

Fig. S14. SEM images of Bi_2Se_3/PP after 100 cycles at 0.2 C

Table S2. Comparison of the capacity retention at various high current density in this work with recently reported Li-S batteries.

Modified materials	Sulfur host	S loading (mg cm^{-2})	Capacity decay rate/cycle number/ C rate	High rate (Initial capacity) (mAh g^{-1} cm^{-2})	Ref.
MoO_2-Mo_2N	CB/S	0.8-1.0	0.088%/300/0.5C	842/2C	[25]
TiO_2/C/BiOBr	S	-	0.194%/300/0.5C	416/2C	[50]
Ni/SiO_2/G	Super P/S	1.0-1.2	0.086%/300/1C	782/2C	[S7]
Co_3Fe_7	-	1.0	0.088%/500/1C	1029/2C	[S8]
TiN	Super P/S	1.3	0.091%/400/1C	672/3C	[S9]
LMO/SP/NF	CNTs/S	1.6	0.090%/500/1C	575.7/3C	[S10]
NbN/G	Super P/S	1.0-1.5	0.096%/300/1C	937/2C	[S11]
Li-MOF/RGO	KB/S	1.2-1.4	0.089%/600/1C	742/2C	[S12]
Co@N-CNTs/N-Mo_xC	KB/S	1.0	0.090%/500/1C	496/5C	[S13]
$NiSe_2$	CNTs/S	1.2	0.089%/500/1C	550.9/4C	[S14]
Pt-NbC-CNT	Super C/S	1.3-1.5	0.088%/500/0.5C	795/5C	[S15]
NWCNT-OH@NH_2-β-CD	KB/S	1.0-1.2	0.087%/800/0.5C	934.5/2C	[S16]
CoNi@MPC	AB/S	1.0-1.5	0.090%/500/1C	665.3/4C	[S17]
Bi_2Se_3	**KB/S**	1.0	**0.086%/500/1C**	**866.3/5C**	**This work**

References:

[S1] G. Kresse and J. Furthmüller, *Phys. Rev. B*, 1996, **54**, 11169–11186.

[S2] G. Kresse and D. Joubert, *Phys. Rev. B*, 1999, **59**, 1758–1775.

[S3] J. P. Perdew, K. Burke and M. Ernzerhof, *Phys. Rev. Lett.*, 1996, **77**, 3865–3868.

[S4] S. Grimme, J. Antony, S. Ehrlich and H. Krieg, *J. Chem. Phys.*, 2010, **132**, 154104.

[S5] J. Shen, X. Xu, J. Liu, Z. Liu, F. Li, R. Hu, J. Liu, X. Hou, Y. Feng, Y. Yu and M. Zhu, *ACS Nano*, 2019, **13**, 8986–8996.

[S6] G. Wang, L. Peng, K. Li, L. Zhu, J. Zhou, N. Miao and Z. Sun, *Comput. Mater. Sci.*, 2021, **186**, 110064.

[S7] C. Chen, Q. Jiang, H. Xu, Y. Zhang, B. Zhang, Z. Zhang, Z. Lin and S. Zhang, *Nano Energy*, 2020, **76**, 105033.

[S8] Z. Gu, C. Cheng, T. Yan, G. Liu, J. Jiang, J. Mao, K. Dai, J. Li, J. Wu and L. Zhang, *Nano Energy*, 2021, **86**, 106111.

[S9] B. Qi, X. Zhao, S. Wang, K. Chen, Y. Wei, G. Chen, Y. Gao, D. Zhang, Z. Sun and F. Li, *J. Mater. Chem. A*, 2018, **6**, 14359–14366.

[S10] T. Li, Y. Li, J. Yang, Y. Deng, M. Wu, Q. Wang, R. Liu, B. Ge, X. Xie and J. Ma, *Small*, 2021, **17**, 2104613.

[S11] H. Shi, Z. Sun, W. Lv, S. Xiao, H. Yang, Y. Shi, K. Chen, S. Wang, B. Zhang, Q.-H. Yang and F. Li, *J. Energy Chem.*, 2020, **45**, 135–141.

[S12] M. Zhou, Y. Li, T. Lei, W. Chen, G. Rao, L. Xue, A. Hu, Y. Fan, J. Huang, Y. Hu, X. Wang and J. Xiong, *Small*, 2021, **17**, 2104367.

[S13] G. Zhao, S. Liu, X. Zhang, Y. Zhang, H. Shi, Y. Liu, L. Hou and C. Yuan, *J. Mater. Chem. A*, 2023, **11**, 1856–1865.

[S14] A.-H. Shao, X.-X. Zhang, Q.-S. Zhang, X. Li, Y. Wu, Z. Zhang, J. Yu and Z.-Y. Yang, *ACS Appl. Energy Mater.*, 2021, **4**, 3431–3438.

[S15] Y. Liu, D. Hong, M. Chen, Z. Su, Y. Gao, Y. Zhang and D. Long, *ACS Appl. Mater. Interfaces*, 2021, **13**, 35008–35018.

[S16] T. Feng, T. Zhao, S. Zhu, Z. Wang, L. Wei, N. Zhang, T. Song, L. Li, F. Wu and R. Chen, *ACS Appl. Mater. Interfaces*, 2021, **13**, 23811–23821.

[S17] R. Luo, Z. Zhang, J. Zhang, B. Xi, F. Tian, W. Chen, J. Feng and S. Xiong, *Small*, 2021, **17**, 2100414.